Available online at www.eccomasproceedia.org
Eccomas Proceedia COMPDYN (2017) 1032-1041

ECCOMAS
Proceedia

COMPDYN 2017
6th ECCOMAS Thematic Conference on
Computational Methods in Structural Dynamics and Earthquake Engineering
M. Papadrakakis, M. Fragiadakis (eds.)
Rhodes Island, Greece, 15–17 June 2017

DETAILED SIMULATION OF THE SHAFT INGATE OF A SHIELD TUNNEL UNDER SEISMIC IMPACT

Jinghua Zhang[1], Qingqiang Meng[2], Xinbin Tu[2], Jian Zhao[2], Mingqing Xiao[3], and Yong Yuan[4]

[1] Department of Geotechnical Engineering, Tongji University
No. 1239, Siping Rd., Shanghai
11zhjh@tongji.edu.cn

[2] Dept. of AC Transmission Project, State Grid Corporation of China
No. 86, Chang'an Avenue, Beijing
qingqiang-meng@sgcc.com.cn, 7544350@qq.com, tuxinbin11891@qq.com

[3] Technology Center, China Railway Siyuan Survey and Design Group Co., LTD.
No. 745, Heping Avenue, Wuhan City
tsyxmq@163.com

[4] State Key Laboratory for Disaster Reduction in Civil Engineering, Tongji University
No. 1239, Siping Rd., Shanghai
yuany@tongji.edu.cn

Keywords: Working Shaft Ingate, Shield Tunnels, Seismic Analysis

Abstract. *Under seismic impact, critical joints, such as connecting passages and working shafts, are the weak points in shield tunnels. Due to the sharp structural change, stress concentration in these parts is more severe than that in the regular tunnels. In order to have a better understanding of the seismic behavior of the working shaft ingate in shield tunnels, a three-dimensional finite element model is constructed based on a utility tunnel built in the north of Suzhou City beneath the Yangtze River. The numerical model is composed of three major parts, namely, the working shaft, the shield tunnel and the surrounding soil. For the sake of a realistic simulation, many details are considered in this model, including tunnel segments, bolts, layered soil, etc. The deformation and the displacement near the ingate are investigated along with the internal forces of the bolts. This numerical study is part of a research project which is aimed at analyzing the seismic performance of the very same utility tunnel in Suzhou. Meanwhile, a shaking table test is due. And many valuable predictions are drawn through the numerical analysis.*

Peer-review under responsibility of the organizing committee of COMPDYN 2017.
doi: 10.7712/120117.5474.17723

1 INTRODUCTION

Much attention is drawn to the seismic performance of underground structures, especially after the collapse of Dakai station during the great Hanshin earthquake in 1995 [1]. And tunnels in Sichuan Province experienced serious damage in the Wenchuan earthquake in 2008 [2]. Hence, it is a very important issue to protect underground structures from seismic impact.

Although it is observed in field investigation that critical joints, such as connecting passages and working shafts, are particularly vulnerable to earthquakes, previous studies on the seismic response of shield tunnels mainly focused on the analysis of regular shield tunnels. [3,4] And due to the sharp geometric changes and the inherent structural complexity, it is almost impossible to develop an analytical method for the seismic analysis of critical joints. Most researchers have taken advantage of numerical methods to solve this problem. [5,6]

In this paper, a three-dimensional finite element model is constructed to study the seismic performance of the working shaft ingate of a shield tunnel. Results from the simulation are helping both the practical engineering design and the follow-up shaking table test.

2 PROJECT DESCRIPTION

The numerical model is based on the Sutong GIL Utility Tunnel Project. The tunnel is going to be excavated beneath the Yangtze River in the north of Suzhou City in Jiangsu Province. The launching shaft, which is on the south bank of the river, is still under construction. The tunnel is designed as a single shield tunnel with an outer diameter of 11.6m. And the length of the tunnel is 5.4km.

According to the geological survey, the surrounding soil of the tunnel is composed of sedimentary soil formations. There are five of them, and silty clay is the main construction environment of the tunnel. The corresponding parameters of the soil layers are listed in Table 1.

Like all the other shield tunnels, there are two working shafts at two tunnel ends. Since the tunnel is crossing the Yangtze River from the south to the north, the launching shaft is built on the south bank. The working shaft alone is 34.0m long, 24.8m wide and 20.8m high. And the underground diaphragm walls extend to the level of 17.0m below the bottom floor of the shaft. The ingate is in the north wall of the shaft, while the south wall is connected to a 140.0m long construction passage with a dip angle of 3 degrees. The construction passage is going to be built by cut-and-cover mothed in four separate sections, of which each has a unique structure pattern. Nonetheless, only the section directedly connected to the shaft will be considered in the numerical model.

	Thickness (m)	Unit Weight (kN/m^3)	Shear Wave Velocity (m/s)	Dynamic Shear Modulus (MPa)
Alluvial Silty Clay	18.5	18.1	110	22.35
Grey Silty Clay	20.7	18.7	177	59.78
Silty Fine Sand	29.7	19.3	276	150.02
Medium Coarse Sand	5.6	19.2	333	217.25
Silty Fine Sand	16.4	20.2	341	239.68
Medium Coarse Sand	19.8	20.1	417	356.65

Table 1: Soil parameters. [7]

3 NUMERICAL MODEL

The numerical model comprises three parts: the soil, the shield tunnel and the working shaft (with one section of the construction passage) as shown in Figure 1 and Figure 2.

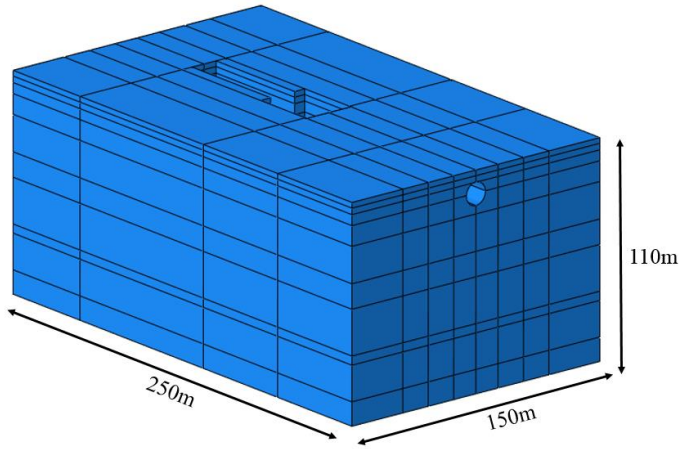

Figure 1: Soil model.

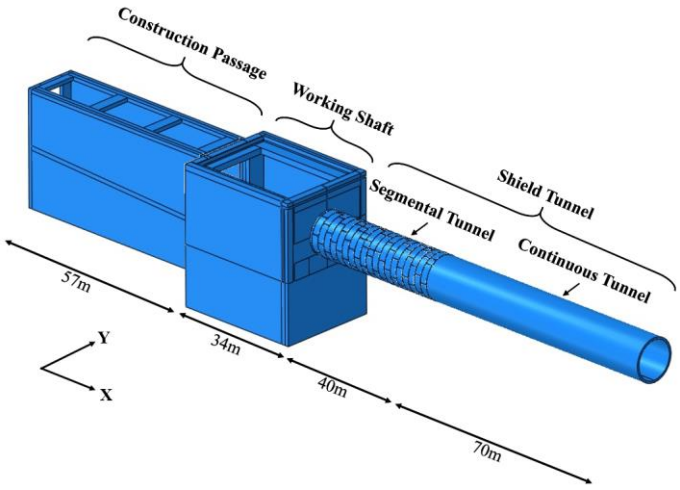

Figure 2: Structure model.

3.1 Soil

As listed in Table 1, the ground soil consists of different strata, so the numerical soil model is partitioned into the same pattern as shown in Figure 1. Each layer of the soil is considered as an elastic, homogeneous, isotropic and continuous body. This is intended to reduce the computation cost on the soil since the soil alone takes up 47% of the number of elements, so that a more detailed numerical tunnel model could be constructed. The soil model is a cuboid with the dimensions of 250.0m long, 150.0m wide and 110.0m high, of which the underside is taken to be the surface of the bedrock. Then a subtraction Boolean operation is applied to the cuboid to make accurate room for the tunnel structures inside. Because of this operation, the soil model has an extremely complicated geometry, especially in the region around the working shaft. Thus, an elaborate meshing scheme is carefully carried out. Each layer of the soil has the corresponding properties listed in Table 1.

3.2 Working shaft

As mentioned above, the working shaft is connected to a construction passage on the south side. In the numerical model, only the section closest to the shaft is considered. Along the longitudinal direction of the tunnel, the shaft alone is 34.0m long and the construction passage is 57.0m long. The material of the structure is C60 concrete in accordance with China's code, which suggests a density of 2500kg/m^3, an elastic modulus of 3.6E4MPa and a Poisson's ratio of 0.3. Both the shaft model and the construction passage model are constructed in unity with the underground diaphragm walls. All the major internal structures are included in the numerical model. The two models are perfectly tied together on their contacting surfaces during the computation, so are the contacting surfaces between the structures and the soil.

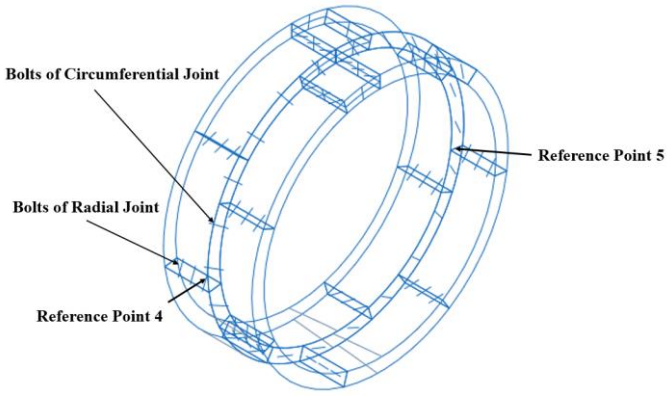

Figure 3: Segmental tunnel ring model.

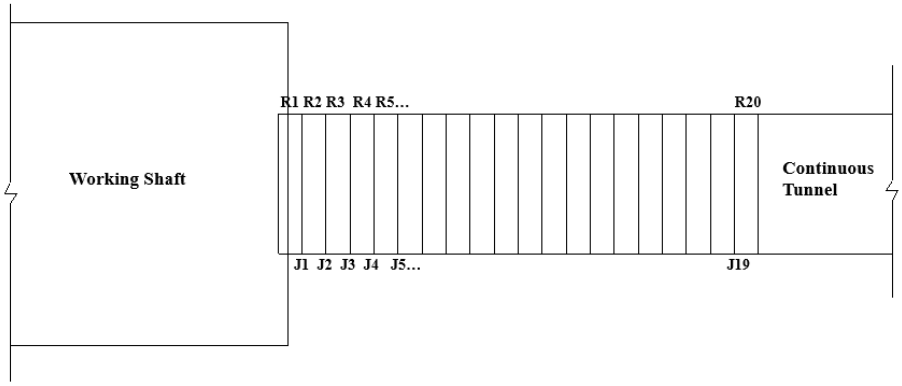

Figure 4: Labels of the segmental tunnel.

3.3 Shield tunnel

The inner and the outer diameters of the original tunnel are 10.5m and 11.6m, respectively. As shown in Figure 2, the length of the shield tunnel model is 110.0m, which amounts to 10 times the diameter of the tunnel. And the tunnel model is a combination of two different structural types. Directly linked to the working shaft is a 40.0m long segmental tunnel. At this region, the numerical model is constructed using the same segments as the actual tunnel. One tunnel ring consists of 8 segments including 1 key segment, 2 adjacent segments and 5 standard segments. Then 20 rings form up the entire segmental tunnel. There are 3 bolts at each radial joint and 22 bolts at each circumferential joint. All the bolts are represented by beam elements and are embedded in the segments. (Figure 3) The material properties of the tunnel segments are the same as the ones of the working shaft model. Next to the segmental region is

a tunnel built up as a continuous pipe. Applying this simplified model could avoid involving too many interacting surfaces in the numerical model, which would require a massive computing power. The continuous tunnel has the same inner and outer diameters as the segmental one while its elastic modulus is timed by a reduction factor of 0.3, because it mainly works as a boundary condition for the segmental tunnel along the longitudinal direction. [8] The interacting circumferential joint of these two regions is also connected by 22 embedded bolts. For the convenience of description, tunnel rings and circumferential joints in the segmental tunnel are labelled from south to north as R1, R2, …, R20 and J1, J2, …, J19, respectively. (Figure 4)

3.4 Interactions

Due to the intricate composition of various model parts, there are many types of interactions in this model.

a) Embedment. All the bolts are embedded in the tunnel linings.

b) Tie. The outside of the working shaft is perfectly tied to the inside of the soil. And the south end of the segmental tunnel is tied to the working shaft.

c) Frictional contact. The outer surface of the shield tunnel and the inner surface of the soil have a frictional contact with a friction coefficient equal to the internal friction coefficient of the soil.

d) Frictionless contact. In the segmental region, the circumferential joints and the radial joints produce over 500 contacting surface pairs. They are all defined as frictionless hard contact.

3.5 Boundary conditions

Since all the tunnel structures are defined to interact with each other or with the surrounding soil, the boundary conditions only concern the soil model. Four side faces of the soil cuboid are free surfaces. The underside of the cuboid is fixed on the vertical direction only. The input seismic wave is Suzhou artificial wave with 2% probability of exceeding in 100 years. (Figure 5) Two cases are computed, in which the acceleration is applied on the underside in two directions. In Case1, the wave is parallel to the tunnel axis. In Case2, the wave is perpendicular to the tunnel axis. It should be noted that gravity is neglected in this model, so the behavior of the structures would be the consequence of the seismic impact alone. Otherwise not only there would be more computing steps but also the results could be interfered.

3.6 Flexible joint

One of the purposes of this study is to examine the effect of flexible joints on the seismic performance of shaft ingate. The most distinguishable characteristic of a flexible joint is that the joint should be able to tolerant large deformation without generating too much stress, which indicates that it is rather a relative concept. In this case, all tunnel segments are linked together by steel bolts. Therefore, flexible joint is simulated by simply reducing the elastic modulus of the bolts. Two models are computed. In the first one, all bolts have an elastic modulus of 2.0E5MPa, so all the joints are “stiff”. This numerical model is called “Model1”. In the second model, one set of the circumferential joint bolts has a smaller elastic modulus of 2.0E4MPa, so it could be considered “flexible”. This model is called “Model2”. The flexible joint is applied to the joint “J1” as shown in Figure 4, namely the closest joint to the ingate. And a third case (Case3) is computed, in which the seismic wave is at a 45-degree angle to the tunnel axis. Results from these two models are extracted and compared.

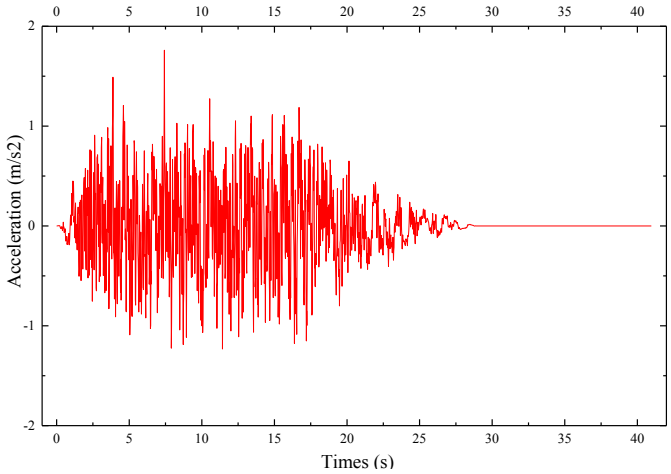

Figure 5: Input acceleration time history. (Peak acceleration 1.76m/s^2)

4 RESULTS

4.1 Seismic response of the shaft

The thickness of the walls of the shaft is 2.4m least. Compared with the shield tunnel, the shaft is relatively stiff, so the seismic behavior of the shaft is very similar to the behavior of a rigid body. Figure 6 is a typical contour of the Mises stress of the working shaft under seismic impact. There is obvious stress concentration around the tunnel ingate. The Mises stress of other parts of the shaft is relatively small and smooth. This agrees with the conclusion that the junction of the shield tunnel and the shaft is most vulnerable to seismic loadings. [3]

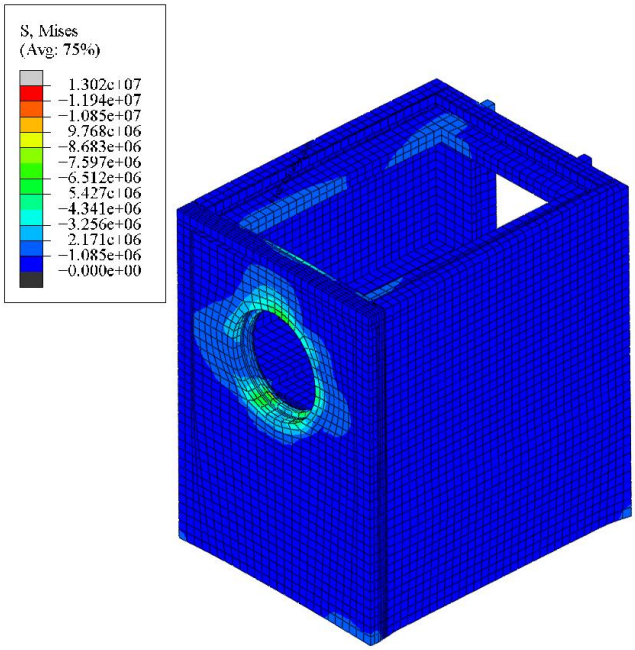

Figure 6: Contour of Mises stress of the working shaft. (Case1, Model1)

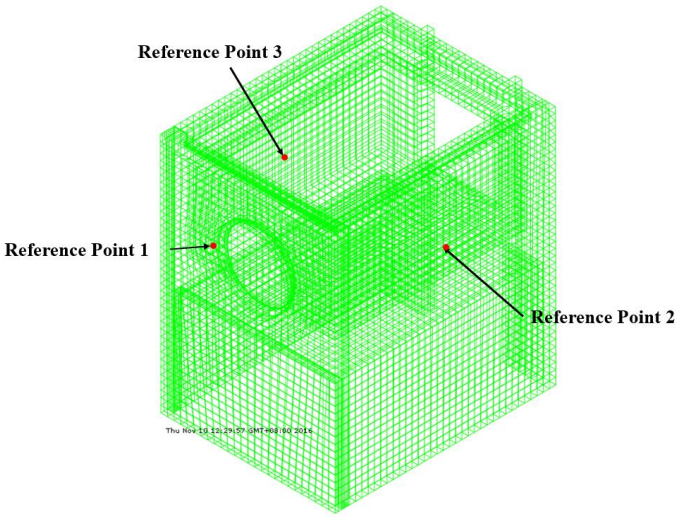

Figure 7: Reference points on the shaft.

To confirm the conclusion observed from the contour, the maximum Mises stress from three reference points (RP) on the working shaft are extracted from two cases and listed in Table 2. The reference points are illustrated in Figure 7. RP1 is from the shaft ingate, while RP2 and RP3 are from the west wall and the east wall, respectively. In both cases, the maximum Mises stress of RP1 is significantly larger than that of the other two points.

		RP1	RP2	RP3
Max Mises Stress (MPa)	Case1	7.84	1.17	1.94
	Case2	5.48	2.52	3.32

Table 2: Maximum Mises stress from three reference points. (Model1)

4.2 Relative displacements at circumferential joints

The shield tunnel is fundamentally an assembly of a large number of tunnel segments connected by bolts. In practical engineering, engineers care about the relative displacements of two segments more than the deformation of the segments. This study is concerned with the relative displacements at the circumferential joints including joint opening and segment dislocation. (Figure 8) At each circumferential joint, two reference points are chosen as shown in Figure3. The displacement data of these two reference points are extracted from J1 to J5. In Case1, the joint openings at these joints are calculated. In Case2, the segment dislocations at these joints are calculated. From J1 to J5, the relative displacements at each joint is plotted in Figure 9. Compared with other joints, J1 is closest to the working shaft ingate, and the joint opening and segment dislocation at J1 are both the largest. The value of the relative displacements at circumferential joints is obviously declining with the joint getting further from the shaft. Expect for joint J1, all the relative displacements are smaller than 5mm.

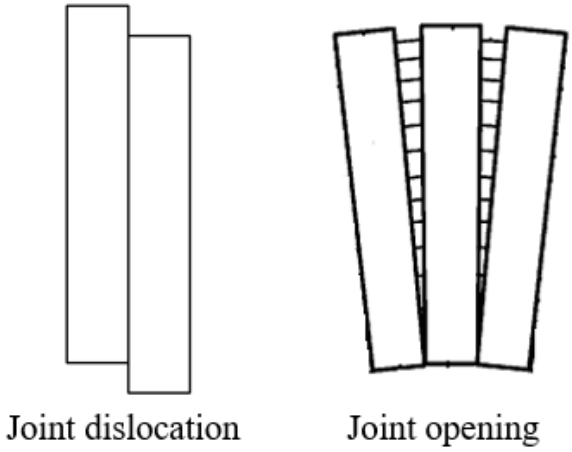

Figure 8: Relative displacement at circumferential joints.

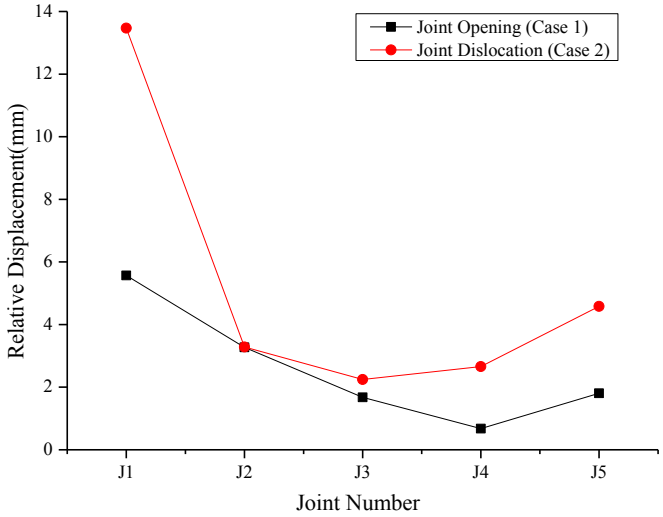

Figure 9: Relative displacements from J1 to J5.

4.3 Effect of the flexible joint

It could be predicted that after the application of the flexible joint, the relative displacements of joint J1 would be increased. In Table 3, the joint opening and the segment dislocation at two reference points are listed. And the data agree with the prediction. The largest increment is 42.22% at RP1. This is easy to understand since the nature of flexible joint is to endure more deformation.

		Model1	Model2	Increment (%)
Reference Point 1	Joint Opening (mm)	0.45	0.64	42.22
	Segment Dislocation (mm)	1.78	1.54	-13.48
Reference Point 2	Joint Opening (mm)	0.76	0.83	9.21
	Segment Dislocation (mm)	2.07	2.90	40.10

Table 3: Relative displacements at two reference points of J1. (Case3)

All the longitudinal bolts (i.e. bolts of circumferential joints) are represented by beam elements. The maximum axial and shear forces of joints J2 to J5 are extracted and listed in Table 4. Only at joint J2, both maximum axial and shear forces are significantly reduced by the flexible joint. At all the other joints, the internal forces are almost identical in two models. The variations are less than 2%. This means that the effective range of the flexible joint is limited to the adjacent joint only. In addition, as shown in Figure 4, ring R1 is tied to the working shaft. The connection between ring R1 and the working shaft has the sharpest structural change, so it must be experiencing the most severe stress concentration. In Model1, the maximum Mises stress of this region is 65.6MPa, while in Model2 it is 64.35 MPa. The maximum Mises stress is barely reduced by the flexible joint (only 1.94%).

	Label	Model1 (kN)	Model2 (kN)	Increment (%)
Axial Force	J2	78.76	70.10	-11.00
	J3	116.20	116.58	0.33
	J4	84.90	84.24	-0.78
	J5	132.52	132.44	-0.06
Shear Force	J2	76.14	70.42	-7.51
	J3	50.80	49.84	-1.89
	J4	44.98	45.04	0.13
	J5	29.72	29.72	0.00

Table 4: Maximum internal forces of longitudinal bolts.

5 CONCLUSIONS

- The working shaft is acting like a rigid body under seismic impact. The deformation of the shaft and its internal structures could be neglected. Meanwhile, the region around the shaft ingate has severe stress concentration.
- The circumferential joint closest to the shaft ingate would have much larger relative displacements during earthquakes than the other joints.
- Relative displacements at the flexible joint could be increased by 42%.
- Flexible joint could significantly reduce the internal forces at the adjacent joint, but it barely affects further ones. And stress concentration at the shaft ingate is not mitigated by the flexible joint.

REFERENCES

[1] K. Uenishi, S. Sakurai, *Characteristic of the vertical seismic waves associated with the 1995 Hyogo-ken Nanbu (Kobe), Japan earthquake estimated from the failure of the Daikai Underground Station,* EE&SD 6(2000): 813–821.

[2] Y. Shen, B. Gao and X. Yang, *Seismic damage mechanism and dynamic deformation characteristic analysis of mountain tunnel after Wenchuan earthquake,* EG 180(2014): 85-98.

[3] A. Koizumi, Seismic damages and case study for shield tunnel (Translated by W. Zhang, D. Yuan) (China Architecture and Building Press, Beijing, 2009). (In Chinese)

[4] K. Kazuhiko, Aseismic Design of Underground Structures. (Kashima Publishing Company, Japan, 1994). (In Japanese)

[5] G. Kong, J. Zhou and S. Wang, *Study on seismic responses of connectional passages for a shield tunnel*, JEEEV 29(2009): 101-107. (In Chinese)

[6] W. Zhao, X. He and W. Chen, *Analysis of seismic damage of segments and joints at the junction of shield tunnel and shaft*, CJRME 31(2012): 3847-3854. (In Chinese)

[7] East China Electric Power Design Institute, Geotechnical Investigation Report of Receiving Shaft on the South Bank (Shanghai, 2016). (In Chinese)

[8] F. Ye, P. Yang and J. Mao, *Longitudinal rigidity of shield tunnels based on model tests,* CJGE 1(2015): 83-90. (In Chinese)